

Microscopic and Spectroscopic Studies of Nanoscale Zero-Valent Iron Supported on Pillared Bentonite

I. A. Ndanusa¹, B. O. Aderemi², A. Hamza², D.B. Hassan³

¹Department of Chemical Engineering, Kaduna Polytechnic, Kaduna, Nigeria

²Department of Chemical Engineering, Ahmadu Bello University, Zaria, Nigeria ³Centre for Energy Research and Training, Ahmadu Bello University, Zaria, Nigeria

Submitted: 10-03-2022

Revised: 21-03-2022

Accepted: 23-03-2022

ABSTRACT: In this study, we synthesized Nanoscale zero-valent iron (nZVI) Composite by ferric iron reduction method using sodium borohydride as a reducing agent under ethanol medium at atmospheric conditions and study its microscopic and spectroscopic structure using XRD, SEM, TEM and FTIR equipment. The XRD micrograph revealed that the material is predominantly Fe⁰ and Fe₂O₃ while the morphology of the obtained iron nanoparticles revealed from TEM micrograph show that it consists of a zero valent core surrounded by oxide shell. The diameter of iron nanoparticles synthesized was 6.23nm with 10nm particle size. In addition, the SEM micrograph and spectra obtained from FTIR further confirmed that synthesis of Fe⁰ was successful with reduce agglomeration.

KEYWORDS: Nano zero-valent iron; nanomaterial modification, pillared bentonite, reducing agents, morphology and micrograph.

I. INTRODUCTION

Nanoscale zero-valent iron, nZVI, (Fe⁰) is a nanomaterial with nanometer length scale (1-100 nm) and specific surface area of about 33.5m²/g with large surface area to volume ratio and enhanced reactivity [1]. The technology of nanoparticle is growing rapidly in the area of scientific research because of their intrinsic properties such as small particle size, large specific surface area, high number of reactive surface sites, high reactivity and mild reaction conditions [2,3]. Although there are variety of nanomaterials such as, iron (Fe⁰), magnesium (Mg⁰), palladium (Pd⁰) and silver (Ag⁰), zeolite (ze⁰) or bimetallic nanoparticles (Fe/Pd, Fe/Ag) which are subject of active research and development in recent time[4,5]. Among them, nano zero valent iron (F⁰)

has become prominent nanomaterials and most extensively applied nanoparticle because of its ability to remove toxic pollutants including organic compounds, inorganic anions and heavy metal ions [6,7]

Although in recent times, the chemical reduction of persistent pollutants using nanoscale zero-valent iron (nZVI) has received much attention due to its smaller particle size, larger specific surface area, higher density of reactive surface sites, and greater intrinsic reactivity of surface sites [8,9]. However, there are still some technical challenges in applications that affect the use of this material in in-situ remediation. These challenges resulted from magnetic properties as they have natural tendency to aggregate which generates significant losses in reactivity and decreases environmental mobility and of course, they are prone to surface oxidation[2]. For instance, the aggregation of nZVI limits its mobility, dispersivity, durability, and mechanical strength, and the oxidization can significantly decrease its reactivity [10,11]. For this reason, nanomaterial surface modification has been a widely studied area and has attracted great attention because it can provide tools to modify the interactions that nano zero valent iron may have with the surrounding environment [6]. Consequently, offering a support for nZVI particles has been considered as an alternative method [12,13].

Pillared clay due to its high surface area and uniform pore structure have been used as effective supports for catalytically active components such as oxides, metals and organometallic complexes [14]. In the past few decades there have been extensive studies on the preparation, characterization and catalytic activity of supported nano zero valent iron on pillared clays

[10,13]. Many of these studies point to the fact that the catalytic efficiency of nanocomposite particles is enhanced significantly when dispersed in the pillared clay matrix [12]. The interaction between the nanomaterial and pillar in the clay microenvironment has been crucial for the stabilization of the nano particles [15]. Over the last few years' different types of nano zero valent iron supported on bentonites intercalated into organic and inorganic cations have been synthesized: Nanoscale zero valent iron supported on pillared clay [2]; nanoscale zero valent iron supported on pillared Al-bent [12]; nanoscale zero valent iron immobilized on organo bentonite [2]; Aluminum Pillared Palygorskite-Supported Nanoscale Zero-Valent Iron [16] etc. However, to the best of our knowledge synthesis of nano zero valent iron supported on Aluminum-iron pillared bentonites is still limited in a peer reviewed journals. The objective of this work was to synthesize nanoscale zero valent iron (Nanocomposite) Supported on Aluminum-iron pillared bentonite using borohydride in liquid-phase reduction method and to investigate its Physicochemical properties using infrared spectroscopy (FTIR), transmission Electron Microscope (TEM), scanning electron microscope (SEM) and X-ray diffraction (XRD).

II. EXPERIMENTAL

2.1. Materials and chemicals

The bentonites used in this study was obtained from Pindiga deposits, Gombe State, Northeast of Nigeria and a simple physical method composed of grinding, dispersion and centrifugation was adopted to purify the sample. The chemical composition was SiO₂: 51 wt.%; Al₂O₃: 15 wt.%; Fe₂O₃: 9.51 wt.%; MgO: 1.05 wt.%; CaO: 1.48 wt.%; K₂O: 2.41 wt.%; Na₂O: 3.51 wt.%; TiO₂: 1.54 wt.%; P₂O₅: 1.03 wt.%; LOI: 10.12 wt.% [17]. Chemicals used in this study were of analytical reagent grade and used as received. Chemicals: Iron(III) chloride hexahydrate (FeCl₃.6H₂O); Aluminum(III) chloride hexahydrate (AlCl₃.6H₂O); sodium borohydride (NaBH₄); absolute Ethanol (C₂H₅OH) and sodium hydroxide (NaOH) were all supplied from Merck India. Distilled water was used to prepared the solutions.

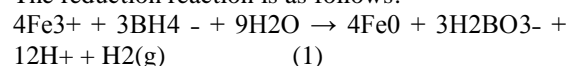
2.2.1 Synthesis of pillared bentonite

The Al-Fe pillared bentonite (AlFe-PILB) was synthesized following an adaptation of the method [18,19,20]. The synthesized was carried out by preparing 0.2 mol L⁻¹ NaOH solution which was added dropwise into a solution of 0.1 mol L⁻¹ AlCl₃ and 0.1 mol L⁻¹ FeCl₃ to prepare pillaring solution of poly (hydroxo (Al³⁺/Fe³⁺)) cations. The pillaring solution was slowly added into 2 g (2% w/w) of

bentonite suspension. The suspension was stirring at 70 °C for 6 h and left to age for 3 days at ambient temperature. The pillared slurry was filtered, washed with distilled water until chloride-free and oven dried at 60 °C for 12 h and calcined at 500 °C for 3 h in a Muffle furnace.

2.2.2. Synthesis of pillared Bentonite-Supported nZVI nanoparticle

Nanoscale zero-valent iron supported on pillared bentonite (nZVI-PILB) was synthesized by ferric iron reduction method using sodium borohydride as a reducing agent under ethanol medium at atmospheric conditions as described by other authors [16, 21]. The preparation consisted of PILB-nZVI with an iron/PILB mass ratio of 1:1. FeCl₃ 6H₂O (4.84 g) was dissolved in 50 mL of miscible liquids (distilled water 80ml and absolute ethanol 20ml at a volume ratio of 4:1), and PILB (2.00 g) was added. The mixture was stirred with magnetic stirrer for 30 min at atmospheric pressure, and then 3.6 g NaBH₄ solution (200 mL) was added to the mixtures and stirred with magnetic stirrer under atmosphere pressure for 1 h to disperse the aluminum-iron pillared bentonite. The black solid materials were separated from the liquid phase via vacuum filtration and rinsed three times with absolute ethanol this is to prevented the nZVI from oxidizing, and then it was dried at 60 °C 5 h. The reduction reaction is as follows:



III. CHARACTERIZATION OF PILLARED BENTONITE-SUPPORTED NZVI NANOPARTICLE

order to determine the physical properties for the synthesized nZVI particles, the material was analyzed using several techniques: X-ray diffraction analysis device (XRD, PANALYTICAL XPERT PRO) using Cu K α radiation ($\lambda = 1.5418 \text{ \AA}$) continuous scanning with PSD Mode measurement temperature 25 °C at a speed of 29° min⁻¹, was used to determine the crystalline structure and composition of the produced particles, the size of the crystallites synthesized was measured using Scherer's Equation; Transmission Electron Microscope (TEM) (HRTEM Technical G2 20 S-TWIN FEI 200 KV TEM) was used to investigate the surface morphology and particle shape structure; Scanning electron microscope (SEM) (NOVA NANO FE-SEM 450 FEI) was used to investigated the structure and morphology of the particles; Fourier-transform infrared spectroscopy (FTIR) (SPECTRUM 2 PERKIN ELMER) was used in other to confirm the functional groups presence in the particles, The

spectra were collected with a resolution of 4 cm^{-1} in the range of $4,000\text{--}400\text{ cm}^{-1}$

IV. RESULTS AND DISCUSSION

4.1 FTIR analysis of pillared bentonite (PILB)

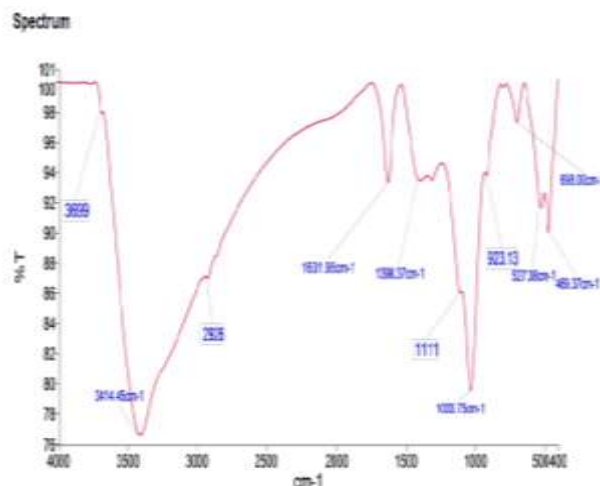


Figure 1: FTIR spectra of the studied pillared bentonite (PILB)

The FTIR spectra of pillared bentonite is shown in Figure 1, It reveals that hydrogen-bonded of water H-O-H and H-O-H deformation at 3414.45 cm^{-1} and 1631.95 cm^{-1} , respectively. The spectral band of 3699 cm^{-1} has been attributed to stretching mode of octahedral O-H groups that attached to Al^{+3} or Mg^{+3} . The Si-O and Si-O-Si groups of the tetrahedral sheet stretching at 796.51 and 1031.80 cm^{-1} respectively. All characteristic vibrational features of the bentonite material are retained in the pillared bentonite. However, the shift of 796.51 cm^{-1} band to 698.00 cm^{-1} , weak band of 527.38 cm^{-1} and presence of a new band at 1111 cm^{-1} show the intercalation of Fe^{3+} and Al^{3+} into bentonite layer. These peaks belonged to characteristic absorption peaks of pillared bentonite

[22,23] and was corroborated by the XRD results Figure 3.

4.2 FTIR analysis of nZVI-PILB

The FTIR spectra of the nZVI-PLB is shown in Figure 2. The bands at 1634 cm^{-1} and the broad high intensity band at 3432 cm^{-1} can be assigned to the H-O-H stretching modes and bending vibration of the free or adsorbed water respectively. The band at 2917 cm^{-1} is associated with the C-H of vinyl groups and the band at 1028 cm^{-1} is associated with the motion of oxygen in Si-O-Si stretch The high-intensity band at 580 cm^{-1} is related to the characteristic absorption peaks of FeO bending vibration [27,28 and 29]. This result revealed that FTIR spectra agreed with XRD peaks and further confirmed that the synthesized particles were predominantly FeO .

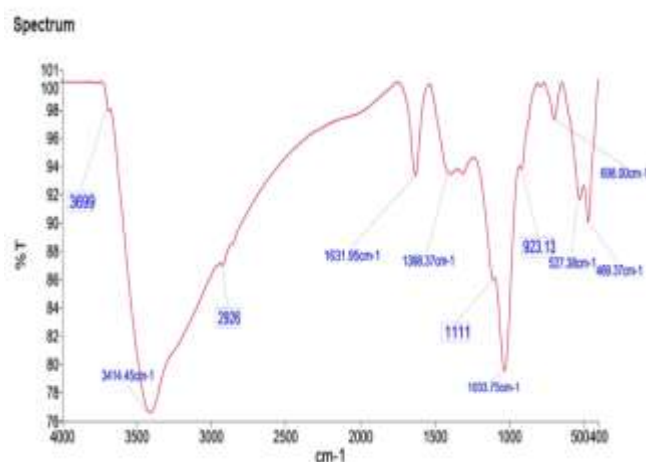


Figure 2: FTIR spectra of the studied nZVI-PILB

4.3 XRD analysis of pillared bentonite

The X-ray diffraction pattern of the pillared sample is presented in Figure 3. As shown in figure 3, suggest that the original bentonite was successfully pillared, presenting a shift from basal reflections at angles 5.8°, 20.95°, 26.75°, 50.20 are characteristic XRD patterns of bentonite [17]. X-ray diffraction provides immediate information

about the success of the intercalation/pillaring process, evidence by shifting of the basal spacing to higher values; usually lower angles in the diffractograms [14]. Therefore, shift in $2\theta^\circ$ suggest increase in basal space which is as a result of intercalation of Al^{3+} and Fe^{3+} into bentonite layer.

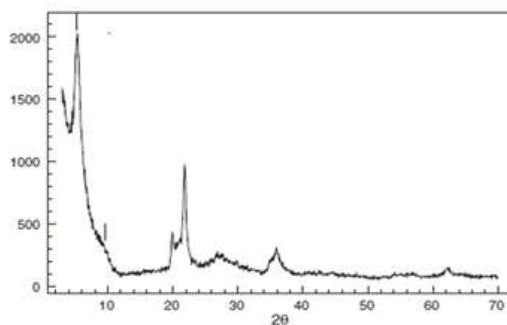


Figure 3: X-ray diffraction pattern for pillared bentonite

4.4.XRD analysis of nZVI-PILB

The X-ray diffraction pattern of the synthesized nZVI-PB particles is shown in Figure 4. The diffraction peaks at (2θ) value of 44.56° indicate the presence of zero-valent iron in agreement with the observation of [26] and low-intensity diffraction peaks at (2θ) value of 36°

reveal that iron was slightly oxidized in PILB [28,31]. The estimated particle size of the nZVI-PB is 15 nm by using the Debye-Scherrer equation which agreed with the result of [29] where he obtained particle size of 10.1 nm for nZVI supported on bentonite.

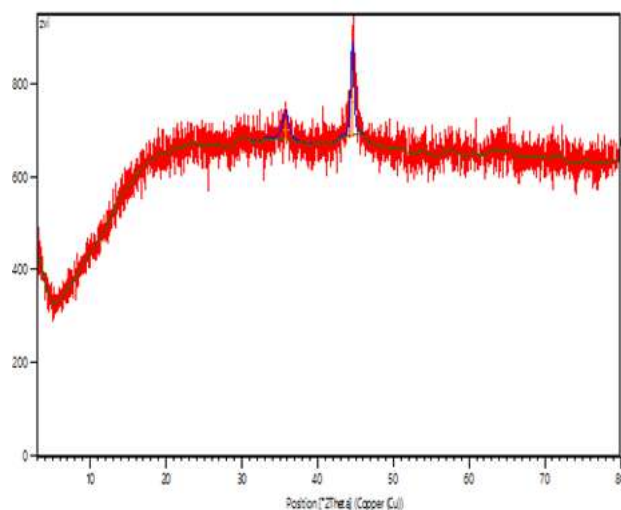


Figure 4: XRD patterns of nZVI supported on PILB

4.5 SEM analysis of nZVI-Supported on PILB

The SEM images of the synthesized PLB-Supported nZVI is shown in Figure 3. The micrograph reveals that nZVI were dispersed on the PLB surface with decreased agglomeration of nZVI which agreed with the observation of [29,30].

Therefore, increase in the surface area of nZVI-PB when compared with PILB. While the decreased agglomeration of nZVI which may be beneficial to more active sites for the catalytic degradation of recalcitrant pollutants

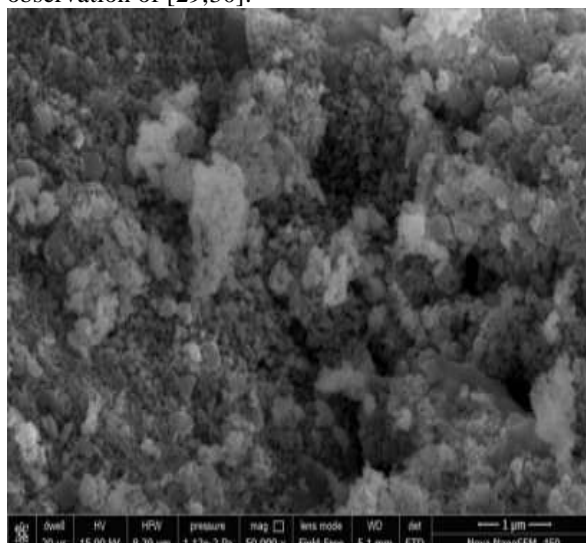


Figure 4.3a: SEM images of nZVI-PILB

4.5 EDX analysis of nZVI-Supported on PILB

Figure. 5. shows the EDX spectra of the nZVI-PILB for the estimation of elemental analysis. The EDX reveals the intense peaks of C (2.07 wt.%), O (24.98 wt.%), Al (1.87 wt.%), Si (2.27 wt.%), Cl (0.90 wt.%) and Fe (67.92 wt.%).

The iron contents in the sample was measured to be 67.92% which confirm that Fe^0 was predominant in the sample. The C and O signals may be attributed to ethanol, while Cl, Al, and Si signals may be attributed to ferric chloride [28,29].

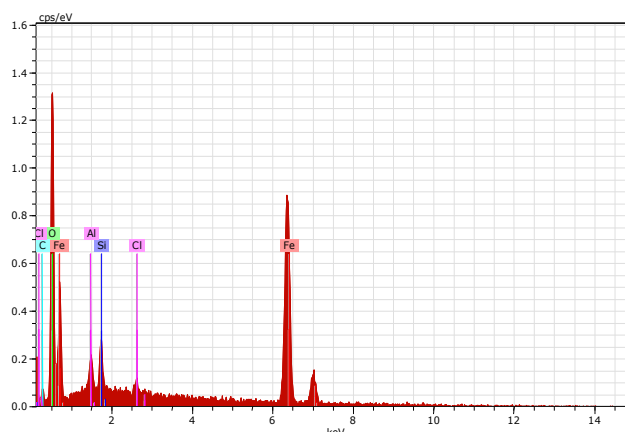


Figure 5: EDX pattern of nZVI-PLB

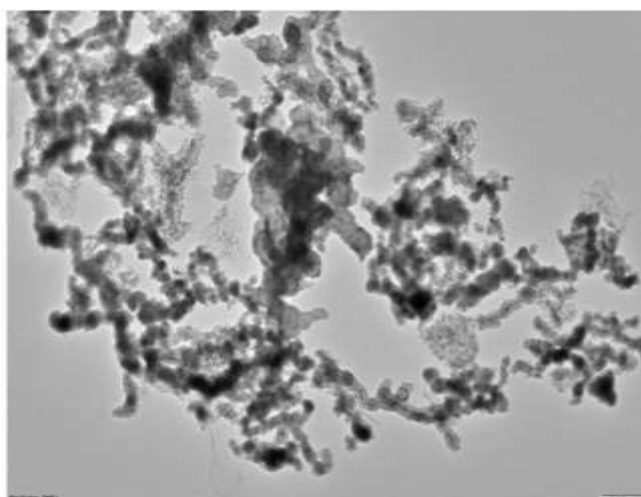
4.6 TEM analysis of nZVI- PILB

The TEM images of the synthesized nZVI-PB is shown in Figure 6. Microscopic morphology of nZVI-PILB shows clearly discrete and well dispersed with decreased agglomeration. As shown in the images the shapes were chain-like structures. Some black particles were supported on chains. The black particles were PILB as supports had been used to prevent aggregation of nZVI particles. This fact is similar to the work of [25] and [13]. In addition, because of the magnetic properties of

nZVI, short needle shaped PILB were connected together to form chainlike structures.

4.7 TEM analysis of core structure and size distribution of nZVI-PILB

The Size distribution analysis in Figure 7 shows that the particle has an average length of 6.445 μm of core. The total particle size measured was 10.1 nm from Figure 7. The total which is in agreement with [13] that reported 10 nm. Fe^0 usually have core shell structure, the core is Fe^0 while the shell layer is Fe_2O_3 .



Figures 6: TEM images of nZVI- PILB

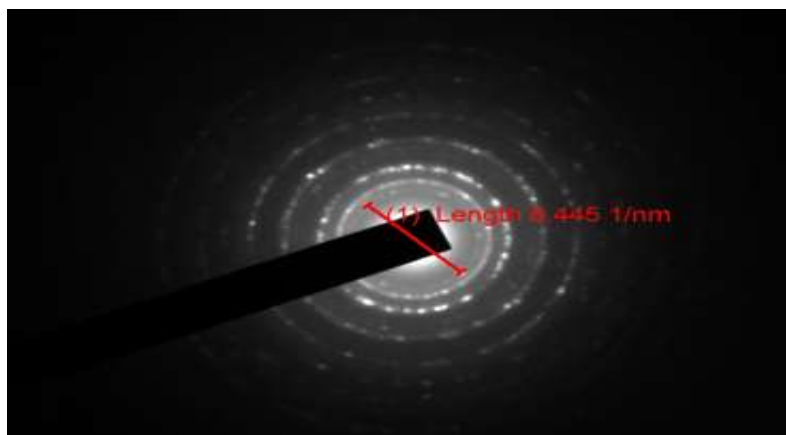


Figure 7. TEM core structure and size distribution of nZVI-PILB

V. CONCLUSIONS

Nanoscaled zero valent iron–supported on pillared bentonite (nZVI-PILB) was successfully synthesized in ethanol medium by borohydride reduction method under atmospheric conditions.. The microscopic and spectroscopic studies of the synthesized nZVI-PILB was carried out using XRD, SEM, TEM, FTIR analysis and it was revealed that iron nanoparticles are predominantly nZVI and that the material form a core-shell model typical of nano zerovalent iron (nZVI). It has a chainlike structure of iron nanoparticles with a particle size of 10 nm. The TEM micrograph indicate that iron nanoparticles consist zero valent core and surrounding an oxide shell with average diameter of 6.23 nm. The SEM micrograph indicate that the synthesized iron nanoparticles have reduce agglomeration when compare with work of [27] and [8] who observed that the synthesised nZVI exhibit some agglomeration and fairly non-uniform particle size with void space. The FTIR revealed that the high-intensity band at 580 cm^{-1} is related to the Fe^0 bending vibration.

Acknowledgements

The authors are thankful to Materials Research Centre Malaviya National Institute of Technology Jaipur, India for the FESEM-EDX, FTIR analysis; Nanoscale Research Facility India Institute of Technology New Delhi, for XRD analysis and Scientium Analyze Solutions Jaipur, India for TEM analysis. The authors greatly appreciate Prof. B.K. Sarma and Dr. Giriraj Tailor of Department of Chemistry, Mewar University Chittorgarh (Rajasthan) India for technical support.

REFERENCES:

- [1]. Adusei-Gyamfi, J., & Acha, V. 2016, "Carriers for nano zerovalent iron (nZVI): Synthesis, application and efficiency".
- [2]. Zheng-xian C, Xiao-ying J, Zuliang C, Mallavarapu M, and Ravendra N. 2011, "Removal of methyl orange from aqueous solution using bentonite-supported nanoscale zero-valent iron", *Journal of Colloid and Interface Science* 363, 601–607
- [3]. Zhanfeng L, Huaping D, Yuling Z, Jianfa L, and Yimin L. 2017, "Enhanced removal of Ni(II) by nanoscale zero valent iron supported on Na-saturated bentonite". *Journal of Colloid and Interface Science*
- [4]. Sanda R, Ivan N, Tea Z. F and Dubravka M. 2019, "Characterization of nZVI nanoparticles functionalized by EDTA and dipicolinic acid". A comparative study of metal ion removal from aqueous solutions, *Royal society of Chemistry advances* 9, 31043
- [5]. Nguyen T. H, Nguyen H. N, L.T, Pham D. K, Tran D. L, and Hoang A. S. 2018, "Preparation and characterization of zerovalent iron nanoparticles". *Vietnam Journal of Chemistry*, 56(2)
- [6]. Yuvakkumara R, Elango V, Rajendrana V, and N. Kannan N. 2011, "Preparation and Characterization of Zero Valent Iron nanoparticles". *Journal of Nanomaterials and Biostructures* Vol. 6, No 4, p. 1771-1776
- [7]. Ramadan E, Osama E, Ahmed M. Khalil E, Bidyut B.S, and Nobuhiro M. 2018, "Improvement of the Chemical Synthesis Efficiency of Nano-scale Zero-valent Iron Particles". *Journal of Environmental Chemical Engineering*.
- [8]. Sravanthi K, Ayodhya D and Yadgiri P.S. 2018, "Green synthesis, characterization of biomaterial-supported zero-valent iron

- nanoparticles for contaminated water treatment". *Journal of Analytical Science and Technology*, 9:3
- [9]. Hee-Chul C, Abul Bashar M. G, and Sushil R. K. 2008, "Method of Synthesizing Air-Stable Zero-Valent Iron Nanoparticles at Room Temperature and Applications"; United States Patent Application Publication
- [10]. Nicolás A, Samuel E. B, Alejandra García, Daniela Muñoz, Pamela S, María A. R, and Dora A. 2016, "Nanoscale zero valent supported by Zeolite and Montmorillonite: Template effect of the removal of lead ion from an aqueous solution". *Journal of Hazardous Materials* 301 371–380
- [11]. Chekli L, Bayatsarmadi B, Sekine R, Sarkar B, Shen A.M, Scheckel K.G, Skinner W, Naidu R, Shon H.K, Lombi E, and Donner E 2015, "Analytical characterization of nanoscale zero-valent iron; methodological review". *Journal of Analytical Chimica Acta*.
- [12]. Yimin L, Jianfa L and Yuling Z 2012, "Mechanism insights into enhanced Cr(VI) removal using nanoscale zero valent iron supported on the pillared bentonite by macroscopic and spectroscopic studies". *Journal of Hazardous Materials* 227– 228: 211– 218
- [13]. Claudio A. R, René F. A, Gabriel A. M, Elpidio M, Tae-Jin L, Hyun-Sang S, Yuhoon H, Abel H and Facundo R 2019, "A cost-effective method to prepare size-controlled nanoscale zero-valent iron for nitrate reduction". *Journal of Environmental Engineering Resources*
- [14]. Molina, C.B., A.H. Pizarro, J.A. Casas and J.J. Rodriguez 2014, "Aqueous-phase hydrodechlorination of chlorophenols with pillared clays-supported Pt, Pd and Rh catalysts". *Applied Catalysis B: Environmental*, 148–149, 330–338.
- [15]. Wen L, Dai C, Zhou X, and Zhang Y 2014, "Application of Zero-Valent Iron Nanoparticles for the Removal of Aqueous Zinc Ions under Various Experimental Conditions". *Plos one* 9(1): *Journal of Catalysis Communications* 11, 937–941
- [16]. Yue, Yuan-yuan H, Ting L, Ying-hao G, and Fei Z 2014, "Aluminum Pillared Palygorskite Supported Nanoscale Zero-Valent Iron for Removal of Cu(II), Ni(II) From Aqueous Solution" *Arab Journal of Science and Engineering*
- [17]. Abdullahi S.L and Audu A. 2017, "Comparative Analysis on Chemical Composition of Bentonite Clays Obtained from Ashaka and Tango Deposits in Gombe State, Nigeria" *ChemSearch Journal* 8(2): 35-40
- [18]. Ksontini N., Najjar W. & Abdelhamid G. 2008, "Al-Fe pillared clays: Synthesis, Characterization and catalytic wet air oxidation activity". *Journal of physics and chemistry of solids* 1112-1115.
- [19]. Nancy S., Andrea A., Rafael M. & Sonia M. 2008, "Synthesis of pillared bentonite starting from the Al-Fe polymeric precursor in solid state, and its catalytic evaluation in the phenol oxidation reaction". *Journal of catalysis today* 530-533.
- [20]. Olaya A., Blanco G., Bernal S., Moreno S. & Molina R. 2009, "Synthesis of pillared clays with Al-Fe and Al-Fe- Ce starting from concentrated suspensions of clay using microwaves or ultrasound, and their catalytic activity in the phenol oxidation reaction, *Journal of applied catalysis B: Environmental* 56-65.
- [21]. Saleh S., Mohammed A. 2020, "Removal of spirinolactone from aqueous solution using bentonite supported nanoscale zero-valent iron and activated charcoal". *Desalination and Water Treatment* 173, 283
- [22]. Zeng-Hui D, Xiang-Rong X, Hui C, Dan J, Yu-Xi Yang, Ling-Jun K, Yu-Xin S, Yong-Xia H, Qin-Wei H, Ling L. 2016, "Simultaneous removal of Cr(VI) and phenol by persulfate activated with bentonite-supported nanoscale zero-valent iron: Reactivity and mechanism". *Journal of Hazardous Materials*
- [23]. Akbar S, and Majid F 2016, "Synthesis of clay-supported nanoscale zero-valent iron using green tea extract for the removal of phosphorus from aqueous solutions". *Chinese journal of chemical engineering; CJCHE* 735
- [24]. Üzümlü Ç, Shahwan T, Eroğlu A.E, Hallam K.R, Scott T.B, and Lieberwirth I (2009, "Synthesis and characterization of kaolinite-supported zero-valent iron nanoparticles and their application for the removal of aqueous Cu²⁺ and Co²⁺ ions". *Journal of Applied Clay Science* 43, 172–181
- [25]. Taha M.R, and Ibrahim A.H 2014, "Characterization of nano zero-valent iron (nZVI) and its application in sono-Fenton process to remove COD in palm oil mill effluent". *Journal of Environmental Chemical Engineering* 2 p1–8

- [26]. Fatemeh A, Ali H and Sirous N 2013, "Surface modification of Fe₃O₄SiO₂ microsphere by silane coupling agent". *Journal of International Nano Letters*, 3:23
- [27]. Niyas A.I, Anbu S, Vikraman G, Nasreen S, M. Muthukumari M and Munish M.K. 2016, "Green Synthesis of Nano Zero valent Iron Particles (nZVI) For Environmental Remediation" *journal of Life Science Archives* Vo 2; 3; p549 – 554
- [28]. Xiaohong G, Yuankui S, Hejie Q, Jinxiang L, Irene M. and Haoran H. 2015, "The Limitations of Applying Zero-Valent Iron Technology in Contaminants Sequestration and the Corresponding Countermeasures": The Development in Zero-Valent Iron Technology in the Last Two Decades, (1994-2014), *journal of Water Research*
- [29]. Yuan-Pang S, Xiao-qin L, Jiasheng C, Weixian Z, Paul H. 2006, "Characterization of zero-valent iron nanoparticles", *Journal of Advances in Colloid and Interface Science* 120, 47–56
- [30]. Yuxian W, Hongqi S, Xiaoguang D, Ha Ming A., Moses O.T and Shaobin W. 2015, "A new magnetic nano zero-valent iron encapsulated in carbon spheres for oxidative degradation of phenol". *journal of Applied Catalysis B: Environmental* 172–173 73–81
- [31]. Djurdja V. Kerkez A., Dragana D. Tomas'evic' A., Ga'bor K., Milena R. Bec'elic' T., Miljana D., Prica C., Srdjan D. Ronc'evic' A., kos K., Boz'o D. Dalmacija A., Zolta'n K. 2014, "Three different clay supported nanoscale zero-valent iron materials for industrial azo dye degradation: A comparative study". *Journal of the Taiwan Institute of Chemical Engineers*